Journal of the Korean Electrochemical Society
Vol. 7, No. 4, 2004, 211-219

REVIEW

A Review of Surface Energy of Solid Electrodes with Emphasis on Its Controversial Issues in Interfacial Electrochemistry

Joo-Young Go and Su-Il Pyun†

Department of Materials Science and Engineering, Korea Advanced Institute of Science and Technology, #373-1 Guseong-dong, Yuseong-gu, Daejeon 305-701, Republic of Korea

(Received September 1, 2004 : Accepted October 25, 2004)

Abstract : A classical Lippmann equation valid for liquid electrodes can not describe the interfacial properties of solid electrodes due to the elastic surface strain on solid electrodes. Although there have been many attempts to derive the thermodynamic equations for solid electrodes during the past few decades, their validity has been still questioned by many researchers. In practice, although there are various experimental techniques to measure surface energy of solid electrodes, the results obtained by each technique are rather inconsistent due to the complexity of the surface strain on solid electrodes. This article covers these controversial issues in surface energy of solid electrodes. After giving brief summaries of the definition of the important thermodynamic parameters and the derivation of the thermodynamic equations for solid electrodes, the several experimental methods were introduced for the measurement of surface energy of solid electrodes. And then we discussed in detail the inconsistent results in the measurement of the potential of zero charge (pzc) and the potential of electrocapillary maximum (ecm).

Key words : Surface energy, Solid electrodes, Thermodynamics, Potential of zero charge (pzc), Electrocapillary maximum (ecm).

1. Introduction

Surface energy of solid electrodes is an important parameter for determining the interfacial properties of solid/liquid interface such as potential of zero charge (pzc), surface charge density, specific adsorption, structures of a double layer and an adsorption layer, *etc*. Since kinetics and mechanisms of electrode processes are considerably affected by the interfacial properties of solid/liquid interface, the deep comprehension of surface energy of solid electrodes is essential to study interfacial electrochemistry.

For liquid electrodes such as mercury, the electrocapillary properties of their surfaces are clearly represented by a classical Lippmann equation.[1] In addition, the precise measurement of surface energy of liquid electrodes is quantitatively conducted under the plastic deformation of liquid electrodes.[1,2] However, for solid electrodes, the classical Lippmann equation is not valid because in this case the surface strain is conjugated to both the plastic and elastic contributions.[3] Therefore, it is very difficult to measure surface energy of solid electrodes owing to its complexity.

In fact, surface energy of solid electrodes has been one of the most controversial topics in interfacial electrochemistry. In thermodynamics, there have been several different methods to derive the thermodynamic equations for solid electrodes, but their correctness and validity has been still questioned by many researchers.[4-9] In practice, although there are various experimental techniques to measure surface energy of solid electrodes, the results obtained by each technique are rather inconsistent, for example, the disagreement of the pzc and the potential of electrocapillary maximum (ecm).[9,10] Therefore, the thermodynamic interpretation is not quite clear of the experimental results obtained from various methods in terms of physical properties of the system.

This paper aimed at reviewing the theoretical and experimental studies on surface energy of solid electrodes and its controversial issues in interfacial electrochemistry. For this purpose, we first summarised the theoretical derivation of the thermodynamic equations valid for any solid electrodes with giving the definition of the important thermodynamic parameters. And then, we introduced several experimental methods for the measurement of surface energy of solid electrodes. Finally, we discussed in detail the controversial issues in surface energy of solid electrodes.

2. Thermodynamics of Solid Surfaces

2.1. Definition of thermodynamic parameters for solid surfaces

Although considerable studies on thermodynamics of solid surfaces have been conducted by many researchers during a few decades, symbols and nomenclature for the thermodynamic parameters of solid surfaces have been still used inconsistently in many articles. In this section, the basic thermodynamic parameters for solid surfaces will be introduced according to the IUPAC recommendations.[11]

2.1.1. Plastic strain ε_p[3]

The surface strain is regarded as plastic when the number

†E-mail: sipyun@webmail.kaist.ac.kr

of molecules in the surface region increases in proportion to the surface area, but the area per surface molecule does not change. For liquid electrodes, the strains in their surfaces are exclusively plastic, because there is no barrier to prevent molecules from migrating to and from the surfaces of liquid electrodes. Plastic strains also arise in solids near their melting points.

2.1.2. Elastic strain ε_e[3)]

The surface strain is regarded as elastic when the number of molecules in the surface region remains constant irrespective of the change in the surface area, but the area occupied by each molecule differs from that in the undistorted case. In the presence of long-range order, the change of the surface area can not be accommodated by migration of molecules to and from the surface, therefore it is elastic.

2.1.3. Superficial work γ^{π}[3,11)]

The superficial work γ^{π} is the reversible work required to form unit area of a new surface by cleavage at constant temperature, pressure, chemical potential, electric field, and elastic strain. The surface strain which results from γ^{π} is purely plastic. γ^{π} is independent of plastic strain at the surface because the new area is the same in nature as the existing area. γ^{π} is a scalar quantity and consequently is isotropic.

2.1.4. Surface stress Υ_{ij}[3,11)]

The surface stress Υ_{ij} is the reversible work required to form unit area of a new surface by stretching with a linear stress, acting in the *j*th direction on an edge normal to the *i*th direction, under equilibrium conditions. The surface strain which results from Υ_{ij} is purely elastic. Υ_{ij} is dependent on elastic strain at the surface because the greater the area changes, the greater do the intermolecular lattice spacings at surface deviate from the equilibrium state.

Υ_{ij} is a tensorial quantity since it is generally anisotropic. For the isotropic solid, the directional dependence of the surface stress disappears, and in this case the surface stress became the half-sum of the diagonal components of the surface stress tensor Υ.

2.1.5. Generalised surface intensive parameter or general specific surface energy γ^s[3,11)]

A generalised surface intensive parameter or a general specific surface energy γ^s is conjugate to the general change of the surface area, which is partly plastic and partly elastic. γ^s is a tensorial quantity. For an isotropic solid, γ^s is formally defined as the sum of the plastic and elastic contributions to the total surface strain ε_{tot} by

$$\gamma^s = \frac{d\varepsilon_p}{d\varepsilon_{tot}}\gamma^{\pi} + \frac{d\varepsilon_e}{d\varepsilon_{tot}}\Upsilon \quad (1)$$

The term of "surface energy of solid electrodes" used in this article means γ^s.

2.2 Thermodynamic equations for solid surfaces

The theoretical works on the derivation of thermodynamic equations for the solid surfaces have intensively been conducted by Shuttleworth,[12)] Herring,[13)] Eriksson[14)] and Couchman,[15-18)] and were reviewed by Linford.[3)] In their works, they assumed that the internal surface energy U^s is a homogeneous function of the first degree involving γ^{π}. It is noted that in general U^s does not involve Υ.[14)] Therefore, ignoring the magnetic and gravitational terms, U^s is expressed by

$$U^s = TS^s - pV^s + \Sigma\mu_i n_i^s + EQ^s + \gamma^{\pi}A \quad (2)$$

where T is the temperature, S^s the surface entropy, p the pressure, V^s the surface volume, μ_i the chemical potential of substance i in the surface, n_i^s the excess amount of substance i in the surface, E the electrode potential, Q^s the surface charge and A represents the surface area.

The first and second laws of thermodynamics allows one to write

$$dU^s = TdS^s - pdV^s + \Sigma\mu_i dn_i^s + EdQ^s + \gamma^s dA \quad (3)$$

By differentiating Eq. (2) and comparing the result with Eq. (3), one finds

$$0 = S^s dT - V^s dp + \Sigma n_i^s d\mu_i + Q^s dE + \gamma^{\pi} dA + Ad\gamma^{\pi} - \gamma^s dA \quad (4)$$

After dividing Eq. (4) by A, one can obtain

$$0 = s^s dT - v^s dp + \Sigma\Gamma_i^s d\mu_i + \sigma dE + \gamma^{\pi} d\varepsilon_{tot} + Ad\gamma^{\pi} - \gamma^s d\varepsilon_{tot} \quad (5)$$

where s^s is the surface excess entropy ($=S^s/A$), v^s the surface excess volume ($=V^s/A$), Γ_i^s the surface excess of substance i ($=n_i^s/A$), σ the charge density on the surface ($=Q^s/A$) and represents the differential of the total surface strain ($=dA/A$).

The total surface strain may be divided into two contributions, *i.e.*, plastic strain and elastic strain,[3,11)] so that

$$d\varepsilon_{tot} = d\varepsilon_p + d\varepsilon_e \quad (6)$$

and substituting Eq. (1) and (6) into Eq. (5) gives

$$0 = s^s dT - v^s dp + \Sigma\Gamma_i^s d\mu_i + \sigma dE + d\gamma^{\pi} + (\gamma^{\pi} - \Upsilon)d\varepsilon_e \quad (7)$$

From Eq. (7), three major thermodynamic equations, namely the Shuttleworth equation,[12)] the Gibbs adsorption equation[3)] and the Lippman equation[1)] may immediately be obtained. In this regard, Linford[3)] called Eq. (7) the most versatile form of the Gibbs-Duhem equation for a surface, *i.e.*, the generalised Gibbs-Duhem equation for a surface.

2.2.1. Shuttleworth equation[3,12)]

The Shuttleworth equation which shows the relationship between γ^{π} and Υ was first derived in a classic paper by Shuttleworth[12)] for solids of threefold or greater symmetry. He obtained from a cyclic approach

$$\Upsilon = \gamma^{\pi} + A\left(\frac{d\gamma^{\pi}}{dA}\right) \quad (8)$$

As Eriksson[14)] originally showed, the final term in Eq. (8) should embody a partial derivative. Couchman *et al.*[15,16)] also revealed that the strain term was solely elastic in nature. Thus, Eq. (8) can be replaced by the following equation which can clearly be obtained from Eq. (7)

$$\Upsilon = \gamma^{\pi} + \left(\frac{d\gamma^{\pi}}{d\varepsilon_e}\right)_{T,p,\mu_i,E} \quad (9)$$

2.2.2. Gibbs adsorption equation[3)]

The generalised Gibbs adsorption equation is easily obtained from Eq. (7) as

$$d\gamma^{\pi} = -s^s dT + v^s dp - \sum \Gamma_i^s d\mu_i - \sigma dE + (\Upsilon - \gamma^{\pi}) d\varepsilon_e \quad (10)$$

If the last two terms of Eq. (10) is omitted, the classical Gibbs adsorption equation is given. In addition, from Eq. (10), it can be seen that γ^{π} is a function of T, p, μ_i, E, and ε_e as stated in the definition of γ^{π} in Section 2.1.3.

2.2.3. Lippmann equation[1,3)]

For purely plastic conditions ($d\varepsilon_e$=0), the partial derivative of the superficial work of solid electrodes with respect to the electrode potential is obtained from Eq. (7) as

$$\left(\frac{\partial\gamma^{\pi}}{\partial E}\right)_{T,p,\mu_i} = -\sigma \quad (11)$$

which is identical to the classical Lippmann equation for liquid electrodes.

In addition, from Eq. (7), the more conventional form of the Lippmann equation involves the quantity $(\partial\gamma^{\pi}/\partial E)_{T,p,\mu_i}$ which is related to σ is given by

$$\left(\frac{\partial\gamma^{\pi}}{\partial E}\right)_{T,p,\mu_i} = -\sigma - (\gamma^{\pi} - \Upsilon)\left(\frac{\partial\varepsilon_e}{\partial E}\right)_{T,p,\mu_i} \quad (12)$$

The magnitude of the second term is highly uncertain, in view of the difficulty of obtaining unambiguous values of Υ and also $(\partial\varepsilon_e/\partial E)_{T,p,\mu_i}$.

2.2.4. Controversial issues in thermodynamics of solid electrodes

It should be noted that Eq. (7) can not be named the Gibbs-Duhem equation because it contains the differential of the extensive parameter ε_e. This is inconsistent with classical thermodynamics stating that the Gibbs-Duhem equation presents the relationship between the intensive parameters in the differential form. This inconsistency is pointed out by Gutman[5)] and Láng and Heusler.[4,7)]

In addition, Láng and Heusler[4,7)] criticised the validity of Eq.(7). They insisted that Eq. (7) can not describe the state of the solid surfaces because the procedure adopted in the derivation of Eq. (7) is incorrect. They pointed out the mistakes in the derivation of Eq. (7) as follows: 1) The Eriksson's assumption,[14)] which means U^s is a homogeneous function of the first order involving γ^{π}, but in general U^s does not involve Υ, is wrong. 2) At equilibrium there is a unique surface energy γ^s which can not be separated into independent contributions from γ^{π} and Υ, *viz.*, Eq. (1) is not valid.

Based on their criticism, they regard U^s as a homogeneous function of the first degree with respect to all extensive variables and then derived new equations for ideally polarisable electrode. In their theory, the classical Lippmann equation is valid in chemical equilibrium. But the deviation from the classical Lippmann equation is expected in the absence of chemical equilibrium. Therefore, they suggested that the deviation from the classical Lippmann equation observed in experimental works originated only from the non-equilibrium between the bulk solid metal and the interphase.

However, recently, Valincius[9)] experimentally verified that the change in the superficial work is uniquely defined by the set of T, p, μ_i, E, and ε_e, and that it does not depend on the path in which the variations of E and ε_e occur. This means that both Υ and γ^{π} are real and definite physical properties. Consequently, Láng and Hueslers insistences are wrong.

3. Methods for the Measurement of Surface Energy of Solid Electrodes

There are various methods for the measurement of surface energy of solid electrodes. Although the generalised surface intensive parameter γ^s is theoretically separated into the plastic and elastic contributions as seen in Eq. (1), in practice two contributions to the total surface strain of solid electrodes can not separately be measured. Therefore, the actual measurement of surface energy of solid electrodes has been conducted under either the purely plastic strain or the purely elastic strain.

Except for a few measurements conducted under the purely plastic deformation,[19-21)] surface energy of solid electrodes has almost been measured where an isotropic solid surface is subjected only to an elastic deformation by such techniques as the extensometer method,[22-25)] the step elastic stretching method under potentiostatic condition,[26)] the quartz oscillator method,[27,28)] the piezoelectric method,[29-43)] the laser beam deflection method (LBDM),[44-55)] the laser interferometry, [56-60)] and the scanning tunneling microscopy (STM).[61-68)] Here, we will introduce the last four techniques which have considerably been used by many researchers and have given the significant results in interfacial electrochemistry.

3.1. Piezoelectric technique[29-43)]

The piezoelectric technique is a powerful method to measure surface energy of solid electrodes. This technique is highly sensitive to a small change in surface energy and is capable of detecting the derivative of surface energy with the electrode potential. A piezoelectric ceramic disk is attached to the back side of the electrode and a small ac voltage is superimposed on a dc electrode potential to produce the change in surface energy, which is converted to electric signals by the piezoelectric ceramic disk and detected by using a lock-in amplifier. The piezoelectric measurement of surface energy of solid electrodes was first developed by Gokhshtein[29)] and further improved by Bard *et al.*[30-32)] and Seo *et al.*[33-42)]

Fig. 1 shows a schematic diagram of the electrode design[30,32)] used in piezoelectric detection of surface energy of solid electrodes. A working electrode was attached to a piezoelectric ceramic disk with epoxy cement. And the piezoelectric ceramic disk was coated by epoxy cement. The working electrode and the piezoelectric ceramic disk were isolated from the piezoelectric ceramic disk and the electrolyte, respectively, by epoxy cement.

A potentiostat connected with a function generator was used

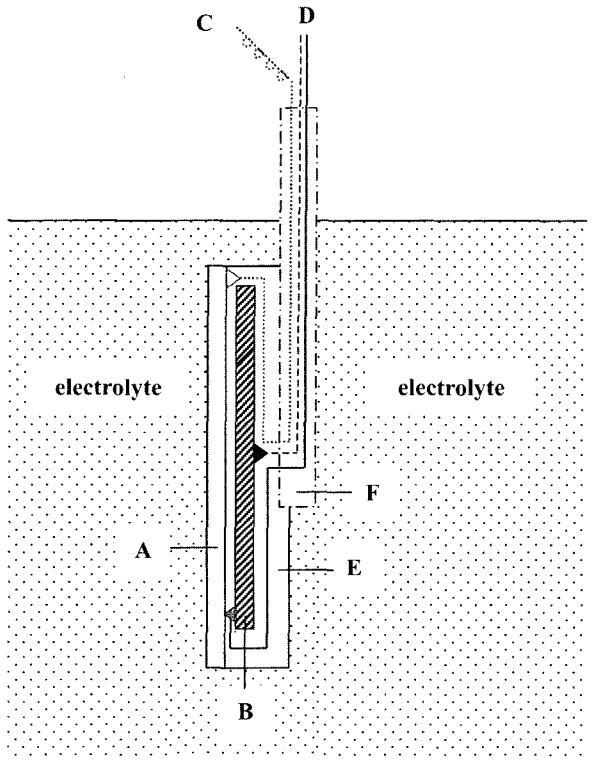

Fig. 1. Schematic diagram of electrode design used in the piezoelectric detection of surface stress of solid electrodes: (A) the working electrode, (B) the piezoelectric ceramic disk, (C) the lead to potentiostat, (D) the leads from piezoelectric ceramic disk to a lock-in amplifier input, (E) the epoxy cement, and (F) the Pyrex glass tube.[30,32]

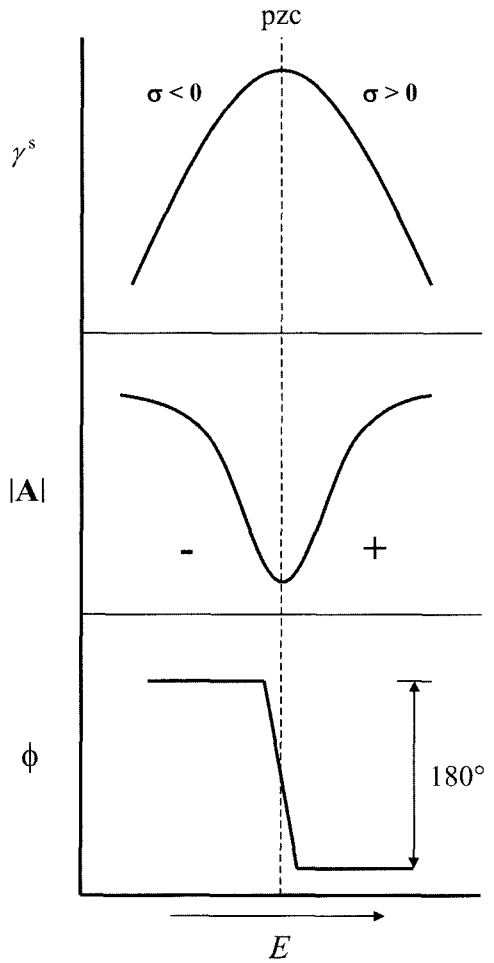

Fig. 2. Relation between piezoelectric signals (|A|: amplitude and ϕ: phase angle) and electrocapillary curve (γ^s vs. E) of sold electrode. σ represents the surface charge density.

to apply to the specimen a linear potential sweep. A sinusoidal signal was superimposed on the linear potential sweep from an oscillator. This small superimposed alternating signal dE induces an alternating change in surface energy $d\gamma^s$ of the working electrode producing corresponding responses from the piezoelectric ceramic disk.

The piezoelectric signals of amplitude |A| and phase angle ϕ were synchronously detected at the same frequency as that of superimposed voltage modulation by using the lock-in amplifier. In principle, |A| is proportional to an absolute value of the derivative of surface energy with the electrode potential $|d\gamma^s/dE|$ and ϕ involves a component of the change in the sign of $d\gamma^s/dE$. However, ϕ involves additional components resulting from the experimental instruments and the mechanical properties of the electrode system. If the contribution of additional components to ϕ is constant, the change in the sign of $d\gamma^s/dE$ could be evaluated from the relative change of ϕ.

Fig. 2 shows schematically the relation between piezoelectric signals (|A| and ϕ) and electrocapillary curve (γ^s *vs.* E). At a maximum of electrocapillary curve, $|d\gamma^s/dE|$ takes a minimum value of zero and the sign of $d\gamma^s/dE$ changes from plus to minus and vice versa. As the corresponding change of piezoelectric signals, |A| takes a minimum value (strictly zero) and ϕ changes relatively by 180°. The potential corresponding to electrocapillary maximum is referred to as the pzc. In practice, the minimum value of |A| likely deviates from zero when the electrical isolation between the working electrode and the piezoelectric ceramic disk is incomplete. Numerical integration of |A| with the electrode potential E by taking the change in the sign of $d\gamma^s/dE$ into account from the relative change of ϕ would gives rise to electrocapillary curve.

3.2. Laser beam deflection method (LBDM)[44-55]

Although the piezoelectric technique is capable of detecting sensitively the changes in surface energy, the measured values have an arbitrary unit from which it seems difficult to derive the surface thermodynamic parameters such as surface charge density and surface excess. Therefore, the measurement of the changes in surface energy $\Delta\gamma^s$ with an absolute unit is needed for better evaluation of the interfacial properties of a solid electrode. Recently, with the help of a position-sensitive photodetector (PSD), $\Delta\gamma^s$ can accurately be measured with the absolute unit by the laser beam deflection method (LBDM). The LBDM has been used to detect $\Delta\gamma^s$ of noble metal electrodes by Fredlein *et al.*[44,45] and Seo *et al.*,[51,52,54] and to measure surface stresses during the anodic oxidation on metals by Pyun *et al.*[46-50,53,55]

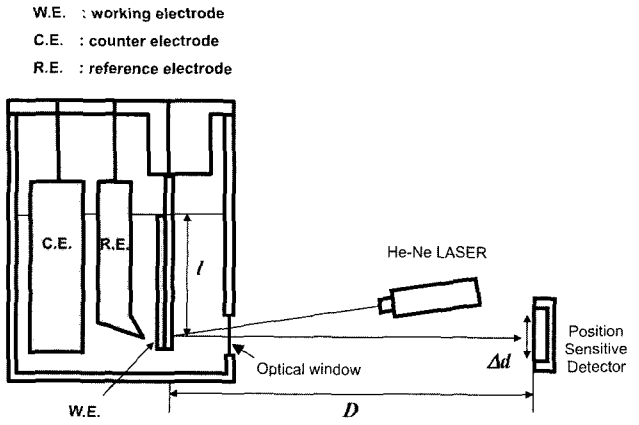

Fig. 3. Schematic illustration for the principle of a laser beam deflection method. *l* is the distance between the solution level and the reflection point of laser beam, *D* the distance between the working electrode (glass substrate) and the PSD, and Δd represents the changes in position of the reflected beam on the PSD.

Experimental apparatus for the LBDM is schematically presented in Fig. 3. The working electrode is prepared by the deposition of a thin film on one-side of a glass substrate. The change in surface energy of the film causes the film electrode to bend and its free end to move. To track this motion a laser beam of He-Ne was directed through a flat window in the side of the cell and reflected off the glass substrate near the end of the electrode. The reflected beam from the glass substrate near the end of the electrode is intercepted by the PSD as a measuring instrument. As the beam moves across the PSD, the position of light spot striking the PSD corresponds linearly to output voltage of the PSD. The changes in output voltage of the PSD were converted into the changes in the position of the reflected beam on the PSD Δd.

Having measured Δd, $\Delta\gamma^s$ developed on the film is given by the Stoney's equation[69] which is combined with Suhir's equation.[70]

$$\Delta\gamma^s = \frac{Y_s t_s^2}{6(1-\nu_s)t_f} \cdot \frac{\Delta d}{2Dl} \tag{13}$$

where Y_s is the Young's modulus of the substrate, t_s the thickness of the substrate, ν_s the Poisson's ratio of the substrate, t_f the thickness of the film, D the distance between the thin glass plate and the PSD, and l represents the distance between the solution level and the reflection point of laser beam.

3.3. Laser interferometry[56-60]

The laser interferometry firstly reported by Jaeckel *et al.*[56] directly measures the elastic deformation of a circular plate due to the changes in surface energy. This method is more sensitive than the quartz oscillator method[27,28] which indirectly determines the changes in surface energy from the detection of the change in the resonant frequency of quartz oscillator. The principle of the laser interferometry is analogous to the LBDM.[44-55]

If a circular AT-cut quartz plate is used, one may simultaneously determine the changes of surface energy, mass, and charge. It was derived[28] from calculations of Janda and Stefan[71] for an unsupported circular AT-cut quartz plate that a change of surface energy is related to the deformation Z* at the centre of the plate with respect to a plane at the radius R by

$$\Delta\gamma^s = \left(\frac{d_Q^2 Z^*}{3R^2}\right)\left\{\frac{(1-\nu_{xy})}{Y_x}\cos^2\varphi + \frac{(1-\nu_{yx})}{Y_y}\sin^2\varphi\right\} \tag{14}$$

in polar coordinates where φ is the angle, d_Q the thickness of the plate, Y_x and Y_y the Young's moduli, and ν_{xy} and ν_{yx} represent the Poisson's coefficients. For the AT-cut, its material constants have the following values: $Y_x = 7.831\times10^{10}$ Pa, $Y_y = 9.066\times10^{10}$ Pa, $\nu_{xy} = 0.277$, and $\nu_{yx} = 0.321$.[71]

Z^* is measured by the laser interferometer, if only the differences of the path of light reflected from the centre of the plate and at some radial distance x shown in Fig. 4 determine the interference pattern. This requirement is fulfilled by the Kösters prism in Fig. 4 showing the Kösters laser interferometer schematically.[56,60]

The 60° Kösters prism (6) is divided in the centre by a semitransparent mirror (5). Light from He-Ne laser is split by a beam splitter (2) into a reference beam and a measuring beam. The beams are chopped at different rates. The measuring beam is reflected by a metal mirror (5) perpendicular to the entrance side of the Kösters prism (6). The point of entrance determines the distance of the two beams emerging from the base of the prism. They are reflected at a nearly zero angle of incidence from the plate. The interfering light leaving the Kösters prism (6) through the exit side, is reflected at the second mirror (5) and then the light is united with the reference beam in the second beam splitter (2). The light is projected onto a screen and a photodiode behind it.

The cylindrical electrochemical cell shown in Fig. 5 contained the working electrode (1) in a specimen holder (2) at the bottom connected by glass tubing (3) to the head of the cell (4) with the counter electrode (8) which was a circular platinum sheet with a central hole for the Luggin capillary (5) and with tubing for the inlet (6) and outlet (7) of the

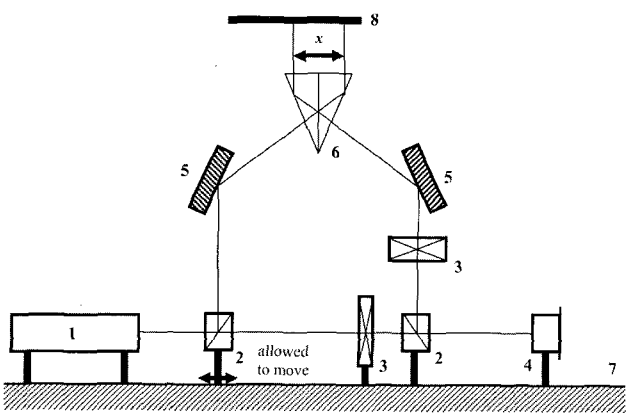

Fig. 4. Interferometric apparatus with (1) the He-Ne laser, (2) the beam divider, (3) the light interrupter, (4) the photodiode, (5) the mirror, (6) the Kösters prism, (7) the optical bench, and (8) the quartz plate.[56,60]

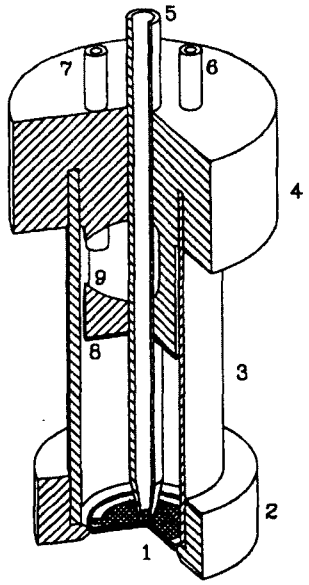

Fig. 5. Electrochemical cell with (1) the working electrode in (2) a specimen holder connected by (3) glass tubing to (4) the head of the cell containing tubings for (5) the Luggin capillary, for (6) the inlet and (7) the outlet of the electrolyte, (8) the counter electrode and (9) a void.[56]

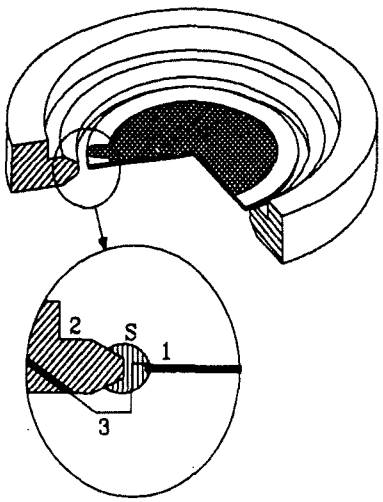

Fig. 6. (1) Quartz oscillator glued with (S) silicone into (2) the quartz holder, and with (3) electrical connections to both electrodes.[56]

electrolyte.

The working electrode was usually one of the gold electrodes sputtered on a thin layer of chromium onto both sides of the polished and flat 10 MHz AT-cut quartz plate after its careful cleaning. If necessary, the gold electrode was covered by some other metal. The second electrode was surrounded at the edge of the plate by an electrically insulated gold ring serving as a mirror in the interferometer. After connecting (with silver paint) both electrodes to copper wires, the quartz plate was glued into the "Trovidur" specimen holder by a ring of silicone rubber as shown Fig. 6. Before use, the silicone was aged at room temperature for at least three weeks. The cell was assembled by first screwing the specimen holder with the glass tubing to the top of the adjustment devices of the interferometer. The head of the cell then was fastened airtight to the top of the cell by glueing with silicone, when necessary.

The device to change the pressure in the cell consisted of U-tubing half filled with pure water. The connection of one leg to the outlet at the head of the cell was filled with nitrogen. Water was pumped into the other leg open to the air by a peristaltic pump. The quartz was oscillated by using the oscillator circuit. The digital data from the counter were transferred by GPIB to a computer. The analogue signals for current and potential from the potentiostat and for the voltage from the photodiode were digitised by a 16 bit AD/DA converter.

3.4. Scanning tunneling microscopy (STM) [61-68]

A direct and accurate method to measure the deflection of the film on the cantilever due to the changes in surface energy of the film is provided by the STM. In fact, the original version of the atomic force microscopy (AFM)[72] was based on the action of the STM. In recent considerations, the STM was also employed for the detection of small displacements.[61] The use of the STM for the direct measurement of electrochemically induced surface energy may be helpful in clarifying some of the controversial aspects concerning the thermodynamic interpretation.

The magnetically inverted operation of the beetle type STM and the electrochemical arrangements are illustrated in Fig. 7. Of particular interest may be the way the specimens (1) were sealed to the bottom of the cylindrical cell. This was achieved by a gasket and clamp, which left the specimen free to deflect. Glass plates were first coated with chromium and then with gold at room temperature in a high vacuum. Before the experiments, the plates were flame-annealed to

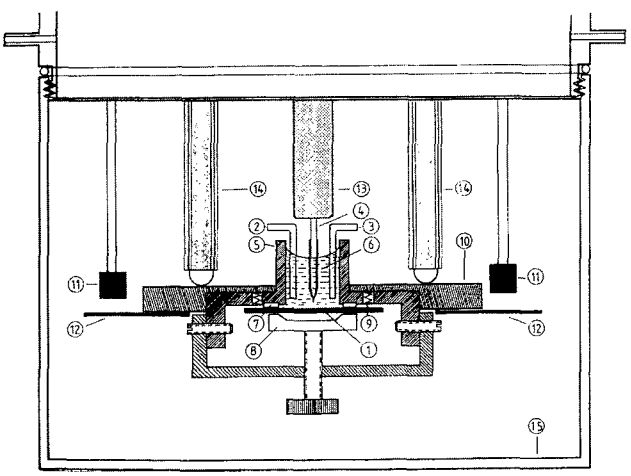

Fig. 7. Schematic illustration of the STM and electrochemical set-up: (1) specimen, (2) the counter electrode, (3) the reference electrode, (4) the tip, (5) the cell, (6) the electrolyte solution, (7) the seal, (8) the screw, (9) the spring, (10) the specimen holder, (11) the magnets, (12) the magnetic iron sheet, (13) the z-piezo, (14) the x-y-piezo, and (15) a housing.[62]

fairly large (111) terraces.[73] The mica substrate was heated to 600 K before evaporation with gold and gently flame-annealed to *ca.* 500 K prior to experiment.

To illustrate how the relative surface energy data were obtained, an STM scan was three-sectioned at the centre of the specimen, corresponding to three different potential, for gold on much stiffer glass substrate. The digitally stored data of such scans were averaged line-by-line to yield the output, such that the first and the last data points on any of the 512 lines were related to the same average potential of that line. By the way, that thermal effect is negligible on the time scale of the experiment.

4. Discussion about Inconsistent Results in Measurement of the Potential of Zero Charge and the Potential of Electrocapillary Maximum of Solid Electrodes

If the new surface of an isotropic solid forms under purely plastic deformation, γ^s is just equal to γ^π, and the classical Lippmann equation of Eq. (11) is valid. On the other hand, γ^s is equal to Υ in the case of the formation of the new surface under purely elastic deformation. From Eqs. (9) and (11), the equation for the isotropic solid electrode in this extreme case is given by

$$\left(\frac{\partial \gamma^s}{\partial E}\right)_{T,p,\mu_i,\varepsilon_e} = \left(\frac{\partial \Upsilon}{\partial E}\right)_{T,p,\mu_i,\varepsilon_e} = -\sigma - \left(\frac{\partial \sigma}{\partial \varepsilon_e}\right)_{T,p,\mu_i,E} \quad (15)$$

Eq. (15) means that the potential of electrocapillary maximum E_{ecm} does not always coincide with the potential of zero charge E_{pzc}, if the second term, $(\partial\sigma/\partial\varepsilon_e)_{T,p,\mu_i,E}$, is not negligibly small compared with σ.

From the experimental works using the piezoelectric method[29] and the extensometer method,[22-24] it was noted that E_{ecm} of polycrystalline gold did not coincide with E_{pzc}. Furthermore, the results obtained from Au(111) and Au(100) in an $HClO_4$ electrolyte by using the STM technique[66] showed the monotonic decrease of surface energy with increasing electrode potential, *viz.*, the ecm did not appear in the potential range where E_{pzc} should be expected. These disagreements between E_{ecm} and E_{pzc} provides the experimental evidences of the fact that the second term in the right-side of Eq. (15) $(\partial\sigma/\partial\varepsilon_e)_{T,p,\mu_i,E}$ is quite comparable with σ in solid electrodes.

However, from the experimental results obtained from the sputtered gold thin films using the LBDM[44,45] and the laser interferometry,[56,57] and from the those results obtained from the Au(111) electrodes on which the underpotential deposition of copper takes place using the STM,[64,65] it was found that E_{ecm} fairly coincided with E_{pzc}. It is worth noting that the measurements performed under purely plastic deformation often demonstrate the coincidence of E_{pzc} with E_{ecm}.[19-21] Therefore, from those works mentioned above, it can be suggested that the classical Lippmann equation can also be valid for solid electrodes since $(\partial\sigma/\partial\varepsilon_e)_{T,p,\mu_i,E}$ is negligibly small compared with σ.

From the above argumentations, it is shown that in practice, the experimental results obtained by various methods for the measurement of surface energy of solid electrodes are greatly inconsistent with each other. Nevertheless, the inconsistency in the measurement of surface energy of solid electrodes has been disregarded or misunderstood by many researchers.

The results of Beck[22] and Lin[23,24] seem extremely interesting because they found that the value of E_{ecm} of gold is always more negative compared to the value of E_{pzc} obtained by using differential capacitance method.[74,75] This trend was observed independently of the nature of electrolyte (SO_4^{2-}, ClO_4^-, NO_3^-, or halide anions).[23,24] Unfortunately, the authors overlooked the difference in value between E_{ecm} and E_{pzc}, and they assigned the value of E_{ecm} found in their experiments to the value of E_{pzc}.

Recently, Valincius[9,10] has attempted to illustrate the controversial issues in surface energy of solid electrodes and he has given a clue to solve these problems clearly. He investigated the elastic electrocapillary properties of polycrystalline gold using the piezoelectric method,[10] and obtained the experimental results consistent with those of Beck[22] and Lin.[23,24] From these results, it is convinced that the classical Lippmann equation is no longer valid for solid electrodes.

In addition, he suggested that for solid metals, the presence of the electric dipole layer is the primary reason for the discrepancy between the value of E_{ecm} and E_{pzc}. According to Valincius,[9,10] the second term in the right-side of Eq. (15) $(\partial\sigma/\partial\varepsilon_e)_{T,p,\mu_i,E}$ originates from the variation of the charge density of solid electrode during the elastic stretching process. $(\partial\sigma/\partial\varepsilon_e)_{T,p,\mu_i,E}$ is positive and almost constant for gold electrode near the pzc and in the potential range $E < E_{pzc}$. In this potential range, a positive term could be associated with the influence of the elastic stretching on the charge density of electronic dipole layer on gold. However, in the potential range $E > E_{pzc}$, $(\partial\sigma/\partial\varepsilon_e)_{T,p,\mu_i,E}$ strongly depends on both concentration of anions in the electrolyte and pH of the electrolyte. From this result, it was suggested that anions appreciably influence structure of the double layer in the potential range $E > E_{pzc}$.

5. Concluding Remarks

The present article first summarised the theoretical derivation of the thermodynamic equations valid for any solid electrodes with giving the definition of the important thermodynamic parameters. And then, this article introduced several experimental methods such as the piezoelectric method, the laser beam deflection method (LBDM), the laser interferometry, and the scanning tunneling microscopy (STM) for the measurement of surface energy of solid electrodes. Finally, this article discussed in detail inconsistent results in measurement of the potential of zero charge and the potential of electrocapillary maximum of solid electrodes.

Consequently, it is recognised that the considerable theoretical and experimental investigations of surface energy of solid electrodes are still necessary to solve clearly its contro-

versial problems in interfacial electrochemistry. Valincius's suggestion that for solid metals, the presence of the electric dipole layer is the primary reason for the discrepancy between the value of E_{ecm} and E_{pzc}[9,10] provide a clue to the deep comprehension of surface energy of solid electrodes. The further studies on surface energy of solid electrodes may be focused on the properties of the electric dipole layer in various system.

Acknowledgements

This work was supported by the Brain Korea 21 project. Additional acknowledgement is given Mr. T.-S. Jang for the start help at preparing this manuscript as a student job at this laboratory.

Nomenclature

A	Surface area (m^2)
$\|A\|$	Piezoelectric signals of amplitude
D	Distance between the thin glass plate and the PSD (m)
d_Q	Thickness of the plate (m)
Δd	Changes in the position of the reflected beam on the PSD
E	Electrode potential (V)
E_{ecm}	Potential of electrocapillary maximum (V)
E_{pzc}	Potential of zero charge (V)
ε_e	Elastic strain
ε_p	Plastic strain
ε_{tot}	Total surface strain
$d\varepsilon_{tot}$	Differential of the total surface strain, dA/A
ϕ	Piezoelectric signals of phase angle
Γ_i^s	Surface excess of substance i, n_i^s/A (mol m^{-2})
γ^x	Superficial work (J m^{-2})
γ^s	Generalised surface intensive parameter or general specific surface energy (J m^{-2} or N m^{-1})
$\Delta\gamma^s$	Changes in surface energy (J m^{-2} or N m^{-1})
Υ	Half-sum of the diagonal components of the surface stress tensor
Υ_{ij}	Surface stress (N m^{-1})
φ	Angle in polar coordinate
l	Distance between the solution level and the reflection point of laser beam (m)
μ_i	Chemical potential of substance i in the surface (J mol^{-1})
n_i^s	Excess amount of substance i in the surface (mol)
ν_s	Poisson's ratio of the substrate
ν_{xy} and ν_{yx}	Poisson's coefficients
p	Pressure (Pa)
Q^s	Surface charge (C)
R	Radius (m)
S^s	Surface entropy, S^s/A (J K^{-1})
s^s	Surface excess entropy, Q^s/A (J K^{-1} m^{-2})
σ	Charge density on the surface, (C m^{-2})
T	Temperature (K)
t_f	Thickness of the film (m)
t_s	Thickness of the substrate (m)
U^s	Internal surface energy (J)
V^s	Surface volume (m^3)
v^s	Surface excess volume, V^s/A (m)
x	Some radial distance (m)
Y_s	Young's modulus of the substrate (Pa)
Y_x and Y_y	Young's moduli (Pa)
Z^*	Deformation of quartz plate (m)
AFM	Atomic force microscopy
ecm	Electrocapillary maximum
LBDM	Laser beam deflection method
PSD	Position-sensitive photodetector
pzc	Potential of zero charge
STM	Scanning tunneling microscopy

References

1. D. C. Grahame, Chem. Rev., **41**, 441 (1947).
2. H. Girault and D. Schiffrin, "Electroanalytical Chemistry", A.J. Bard (Ed.), 15, 2, Marcel Dekker, New York (1989).
3. R. G. Linford, *Chem. Rev.*, **78**, 81 (1978).
4. G. Láng and K.E. Heusler, *J. Electroanal. Chem.*, **377**, 1 (1994).
5. E. M. Gutman, *J. Phys.: Condens. Matter*, **7**, L663 (1995).
6. R. Guidelli, *J. Electroanal. Chem.*, **453**, 69 (1998).
7. G. Láng and K.E. Heusler, *J. Electroanal. Chem.*, **472**, 168 (1999).
8. R. Guidelli, *J. Electroanal. Chem.*, **472**, 174 (1999).
9. G. Valincius, *J. Electroanal. Chem.*, **478**, 40 (1999).
10. G. Valincius, *Langmuir*, **14**, 6307 (1998).
11. S. Trasatti and R. Parsons, *Pure Appl. Chem.*, **58**, 437 (1986).
12. R. Shuttleworth, *Proc. Phys. Soc. A*, **63**, 444 (1950).
13. C. Herring, "Structure and Properties of Solid Surfaces", R. Gomer and C. W. Smith (Eds.), 3, 5, University of Chicago Press, Chicago (1952).
14. J. C. Eriksson, *Surf. Sci.*, **14**, 221 (1969).
15. P. R. Couchman, W. A. Jesser, D. Kuhlmann-Wilsdorf, and J. P. Hirth, *Surf. Sci.*, **33**, 429 (1972).
16. P. R. Couchman and W. A. Jesser, *Surf. Sci.*, **34**, 212 (1973).
17. P. R. Couchman, D. H. Everett, and W. A. Jesser, *J. Colloid Interface Sci.*, **52**, 410 (1975).
18. P. R. Couchman and D. H. Everett, *J. Electroanal. Chem.*, **67**, 382 (1976).
19. R. S. Perkins, R. C. Livingstone, T. N. Anderson, and H. Eyring, *J. Phys. Chem.*, **69**, 3329 (1965).
20. D. D. Bodé, T. N. Anderson, and H. Eyring, *J. Phys. Chem.*, **71**, 792 (1967).
21. A. Frumkin, "Potential of Zero Charge", Nauka, Moscow, 1979.
22. T. R. Beck, *J. Phys. Chem.*, **73**, 466 (1969).
23. K.-F. Lin and T. R. Beck, *J. Electrochem. Soc.*, **123**, 1145 (1976).
24. K.-F. Lin, *J. Electrochem. Soc.*, **125**, 1077 (1978).
25. T. R. Beck and K.-F. Lin, *J. Electrochem. Soc.*, **126**, 252 (1979).
26. T. Agladze and A. Podobayev, *Electrochim. Acta*, **36**, 859 (1991).
27. A. Grzegorzewski and K. E. Heusler, *J. Electroanal. Chem.*, **228**, 455 (1987).
28. K. E. Heusler and J. Pietrucha, *J. Electroanal. Chem.*, **329**, 339 (1992).
29. A. Y. Gokhshtein, *Electrochim. Acta*, **15**, 219 (1970).
30. R. E. Malpas, R. A. Fredlein, and A. J. Bard, *J. Electroanal. Chem.*, **98**, 171 (1979).
31. R. E. Malpas, R. A. Fredlein, and A. J. Bard, *J. Electroanal. Chem.*, **98**, 339 (1979).
32. L. J. Handley and A. J. Bard, *J. Electrochem. Soc.*, **127**, 338 (1980).
33. M. Seo, T. Makino, and N. Sato, *J. Electrochem. Soc.*, **133**, 1138

(1986).
34. M. Seo, X. C. Jiang, and N. Sato, *J. Electrochem. Soc.*, **134**, 3094 (1987).
35. M. Seo, X. C. Jiang, and N. Sato, *Electrochim. Acta*, **34**, 1157 (1989).
36. X. C. Jiang, M. Seo, and N. Sato, *Corros. Sci.*, **31**, 319 (1990).
37. X. C. Jiang, M. Seo, and N. Sato, *J. Electrochem. Soc.*, **137**, 3804 (1990).
38. X. C. Jiang, M. Seo, and N. Sato, *J. Electrochem. Soc.*, **138**, 137 (1991).
39. M. Seo and M. Aomi, *J. Electrochem. Soc.*, **139**, 1087 (1992).
40. M. Seo and M. Aomi, *J. Electroanal. Chem.*, **347**, 185 (1993).
41. M. Seo, M. Aomi and K. Yoshida, *Electrochim. Acta*, **39**, 1039 (1994).
42. M. Seo and K. Ueno, *J. Electrochem. Soc.*, **143**, 899 (1996).
43. G. Valincius and V. Reipa, *J. Electrochem. Soc.*, **147**, 1459 (2000).
44. R. A. Fredlein, A. Damjanovic, and J. O'M. Bockris, *Surf. Sci.*, **25**, 261 (1971).
45. R. A. Fredlein and J. O'M. Bockris, *Surf. Sci.*, **46**, 641 (1974).
46. J.-D. Kim, S.-I. Pyun, and R. A. Oriani, *Electrochim. Acta*, **40**, 1171 (1995).
47. S.-I. Pyun, J.-D. Kim, and R. A. Oriani, *Mater. Sci. Forum*, **185-188**, 407 (1995).
48. J.-D. Kim, S.-I. Pyun, and R. A. Oriani, *Electrochim. Acta*, **41**, 57 (1996).
49. S.-I. Pyun, *Mater. Lett*, **27**, 297 (1996).
50. S.-M. Moon and S.-I. Pyun, *Electrochim. Acta*, **43**, 3117 (1998).
51. K. Ueno and M. Seo, *J. Electrochem. Soc.*, **146**, 1496 (1999).
52. G. G. Láng, K. Ueno, M. Úvári, and M. Seo, *J. Phys. Chem. B*, **104**, 2785 (2000).
53. K. Ueno, S.-I. Pyun, and M. Seo, *J. Electrochem. Soc.*, **147**, 4519 (2000).
54. M. Seo and Y. Serizawa, *J. Electrochem. Soc.*, **150**, E472 (2003).
55. J.-D. Kim, S.-I. Pyun, and M. Seo, *Electrochim. Acta*, **48**, 1123 (2003).
56. L. Jaeckel, G.. Láng, and K. E. Heusler, *Electrochim. Acta*, **39**, 1031 (1994).
57. G. Láng and K. E. Heusler, *J. Electroanal. Chem.*, **391**, 169 (1995).
58. G. Láng and K. E. Heusler, *Russian J. Electrochem.*, **31**, 759 (1995).
59. I. O. Efimov and K. E. Heusler, *J. Electroanal. Chem.*, **414**, 75 (1996).
60. K. E. Heusler and G. Láng, *Electrochim. Acta*, **42**, 747 (1997).
61. T. W. Kenny, W. J. Kaiser, J. A. Podosek, H. K. Rockstad, J. K. Reynolds, and E. C. Vote, *J. Vac. Sci. Technol. A*, **11**, 797 (1993).
62. W. Haiss and J. K. Sass, *J. Electroanal. Chem.*, **386**, 267 (1995).
63. H.-J. Butt, *J. Colloid Interface Sci.*, **180**, 251 (1996).
64. W. Haiss and J. K. Sass, *J. Electroanal. Chem.*, **410**, 119 (1996).
65. W. Haiss and J. K. Sass, *Langmuir*, **12**, 4311 (1996).
66. H. Ibach, C. E. Bach, M. Giesen, and A. Grossmann, *Surf. Sci.*, **375**, 107 (1997).
67. W. Haiss, R. J. Nichols, J. K. Sass, and K. P. Charle, *J. Electroanal. Chem.*, **452**, 199 (1998).
68. W. Haiss, *Rep. Prog. Phys.*, **64**, 591 (2001).
69. G. G. Stoney, *Proc. R. Soc. Lond. A*, **82**, 172 (1909).
70. E. Suhir, *J. Appl. Mech.*, **55**, 143 (1988).
71. M. Janda and O. Stefan, *Thin Solid Films*, **112**, 127 (1984).
72. G. Binning, C. F. Quate, and Ch. Gerber, *Phys. Rev. Lett.*, **56**, 930 (1986).
73. W. Haiss, D. Lackey, and J. K. Sass, *J. Chem. Phys.*, **95**, 2193 (1991).
74. J. Clavilier and N. Van Houng, *J. Electroanal. Chem.*, **41**, 193 (1973).
75. J. Clavilier and N. Van Houng, *J. Electroanal. Chem.*, **80**, 101 (1977).